  Bull. Chem. Soc. Jpn., 56, 1223—1226 (1983)

Studies on Salt Hydrate for Latent Heat Storage, II. Eutectic Mixture of Pseudo-binary System $CH_3CO_2Na \cdot 3H_2O$-$CO(NH_2)_2$

Takahiro WADA,* Fumiko KIMURA, and Ryoichi YAMAMOTO

Material Research Laboratory, Matsushita Electric Industrial Co. Ltd., 1006 Kodama, Osaka 571

(Received July 5, 1982)

With a view of developing latent heat storage materials, mixtures of pseudo-binary system, $CH_3CO_2Na \cdot 3H_2O$-$CO(NH_2)_2$ (sodium acetate trihydrate–urea) were subjected to differentital scanning calorimetry, and the partial phase diagram for ternary system CH_3CO_2Na–$CO(NH_2)_2$–H_2O at ambient pressure was constructed. The eutectic mixture, containing 0.6 mass fraction of $CH_3CO_2Na \cdot 3H_2O$ and 0.4 mass fraction of $CO(NH_2)_2$, melts congruently at 31.5 °C with a heat of fusion of 226 J/g, which is larger than the heat of fusion of $CaCl_2 \cdot 6H_2O$, 180 *J/g*. Thus, mixtures of system $CH_3CO_2Na \cdot 3H_2O$–$CO(NH_2)_2$ are promising for solar energy storage.

Recently, some mixtures containing salt hydrate have been studied in order to develop latent heat storage materials. Böer *et al.*[1] used a eutectic mixture of system $Na_2SO_4 \cdot 10H_2O$–NH_4Cl–NaCl as a heat storage material for a solar house "solar one." Yoneda and Takanashi[2] studied on mixtures of system $Mg(NO_3)_2 \cdot 6H_2O$–$MgCl_2 \cdot 6H_2O$ and found that the eutectic mixture of this system melts at 59.1 °C and that its heat of fusion is 144 J/g.

In contrast, no mixtures of salt hydrate and organic compound have yet been studied. In this study, mixtures of pseudo-binary system $CH_3CO_2Na \cdot 3H_2O$–$CO(NH_2)_2$ were subjected to measurements using differential scanning calorimetry (DSC). From these measurements, the partial phase diagram for ternary system CH_3CO_2Na–$CO(NH_2)_2$–H_2O at ambient pressure was constructed and the heat of fusion of the eutectic mixture was determined. The linear velocity of the crystallization from pseudo-binary molten mixtures of system $CH_3CO_2Na \cdot 3H_2O$–$CO(NH_2)_2$ was measured and the microstructure of the mixtures was observed and photographed. From the experimental results, we conclude that the $CH_3CO_2Na \cdot 3H_2O$–$CO(NH_2)_2$ mixture is suitable for solar energy storage.

Experimental

Materials. $CH_3CO_2Na \cdot 3H_2O$, CH_3CO_2Na, $CO(NH_2)_2$, and $Na_4P_2O_7 \cdot 10H_2O$ were obtained commercially. $Na_4P_2O_7 \cdot 10H_2O$ was ground and passed through a 100 mesh sieve before use.

Differential Scanning Calorimetry. Differential scanning calorimetry (DSC) was performed with an SSC 560U DSC (Dainiseikosha Co.), a heat flux DSC. Weighed quantities of $CH_3CO_2Na \cdot 3H_2O$, $CO(NH_2)_2$, *etc.* were heated and mixed to a homogeneous melt. One drop of this melt was placed in a 15 μl silver crucible and was solidified. After the crucible was closed, the sample was heated at the rate of 0.5 °C/min from 10 °C to 90 °C. The melting temperature of the sample was obtained from the endothermic peak on the sample temperature curve. The heat of fusion was obtained from the endothermic peak area. This DSC system was calibrated by using ice (t_m: 0.0 °C; ΔH_m: 335 J/g), sodium sulfate decahydrate (t_m: 32.4 °C), and sodium acetate trihydrate (t_m: 58.4 °C) as standards.

Microscopic and Microphotographic Studies. For microscopic and microphotographic studies, slides were prepared and examined under a microscope. A very small drop of melt was placed on a slide and covered with a cover glass. Nucleation was started from one side.

Linear Velocity of Crystallization. The experimental technique for determining the linear velocity of crystallization was similar to that adopted by Dietz *et al.*[3] Measurement was made in a Pyrex glass tube, 500 mm in length, 1 mm in wall thickness, and 8 mm in inner diameter, provided with two right-angled bends. The tube was placed in a water bath thermostated to ±0.1 °C. The melt was seeded at one end and the time required for the crystal boundary to move a definite distance was measured by a stopwatch. The linear velocity of crystallization was determined for various degrees of supercooling in this manner.

Results and Discussion

The phase diagram for binary system CH_3CO_2Na–H_2O based on Greem's data[4] is shown in Fig. 1. In this figure, W_a shows the mass fraction of CH_3CO_2Na and W_b the mass fraction of H_2O. Therefore, the quantity on the abscissa, $100 \times W_a/(W_a+W_b)$, is the weight per cent of CH_3CO_2Na in the system. We see that $CH_3CO_2Na \cdot 3H_2O$ melts incongruently to an aqueous solution containing 58% CH_3CO_2Na by weight in equilibrium with the balance of CH_3CO_2Na as solid anhydrate, and that the balance of CH_3CO_2Na as solid anhydrate dissolves entirely in its water of crystallization at 78 °C.

DSC curves for some mixtures of pseudo-binary system

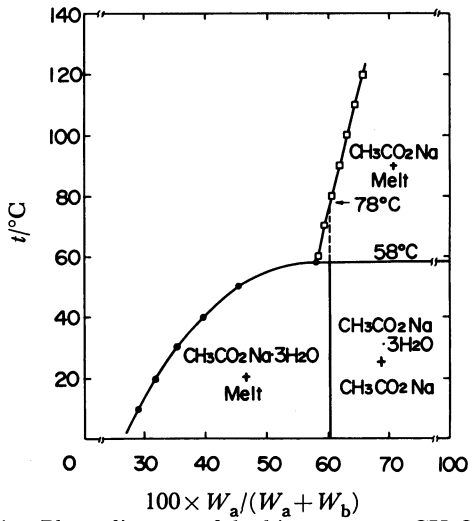

Fig. 1. Phase diagram of the binary system CH_3CO_2Na–H_2O. ●: Melting point of $CH_3CO_2Na \cdot 3H_2O$, □: melting point of CH_3CO_2Na.

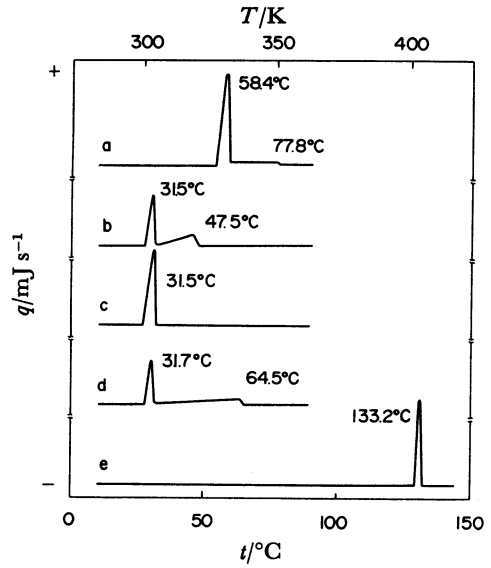

Fig. 2. DSC curves of mixtures of the pseudo-binary system $CH_3CO_2Na \cdot 3H_2O$–$CO(NH_2)_2$. a: $CH_3CO_2Na \cdot 3H_2O$, b: 0.2 mass fraction of $CO(NH_2)_2$, c: 0.4 mass fraction of $CO(NH_2)_2$, d: 0.6 mass fraction of $CO(NH_2)_2$, e: $CO(NH_2)_2$.

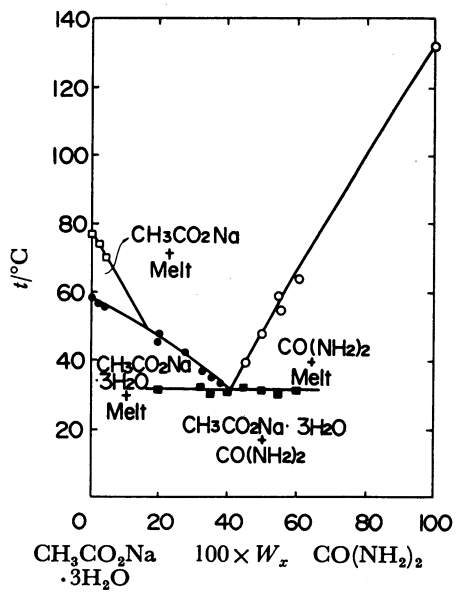

Fig. 3. Pseudo-binary section in a ternary system CH_3CO_2Na–$CO(NH_2)_2$–H_2O at ambient pressure. ●: Melting point of $CH_3CO_2Na \cdot 3H_2O$, ○: melting point of $CO(NH_2)_2$, □: melting point of CH_3CO_2Na, ■: eutectic point.

$CH_3CO_2Na \cdot 3H_2O$–$CO(NH_2)_2$ are illustrated in Fig. 2. Considering the phase diagram of the system $CH_3CO_2Na \cdot H_2O$ shownin Fig. 1, we understand that the peak at 58.4 °C on the DSC curve for $CH_3CO_2Na \cdot 3H_2O$ corresponds to the melting of $CH_3CO_2Na \cdot 3H_2O$ and that the change at 77.8 °C in the DSC curve for $CH_3CO_2Na \cdot 3H_2O$ corresponds to the entire dissolution of the CH_3CO_2Na as solid anhydrate in the water of crystallization.

The pseudo-binary section in ternary system CH_3CO_2Na–$CO(NH_2)_2$–H_2O at ambient pressure which is constructed from such DSC curves is shown in Fig. 3.

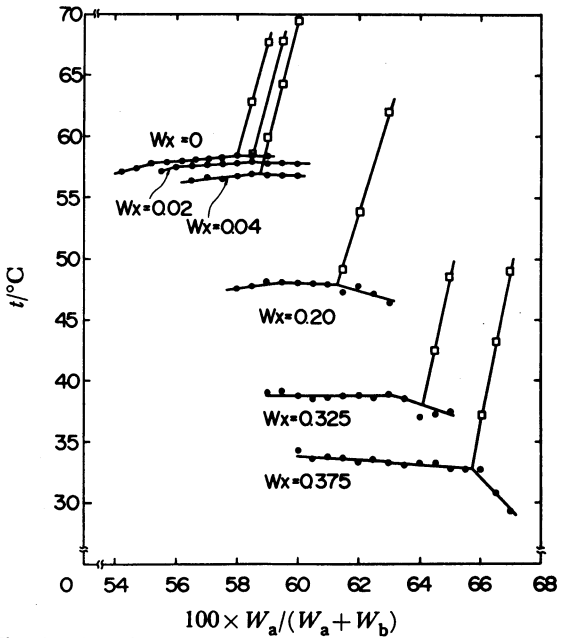

Fig. 4. Melting-point diagram of the ternary system, CH_3CO_2Na–$CO(NH_2)_2$–H_2O, at ambient pressure without $CO(NH_2)_2$ content. ●: Melting point of $CH_3CO_2Na \cdot 3H_2O$, □: melting point of CH_3CO_2Na.

This pseudo-binary section is confirmed by the cooling method adopted by Carlson *et al.*[5] In this figure, W_x shows the mass fraction of $CO(NH_2)_2$, so the quantity on the abscissa $100 \times W_x$ indicates the weight per cent of $CO(NH_2)_2$ in the system. From this figure, it is clear that pseudo-binary system $CH_3CO_2Na \cdot 3H_2O$–$CO(NH_2)_2$ forms a eutectic mixture without forming any new addition compounds. The eutectic mixture of this system, containing 0.6 mass fraction of $CH_3CO_2Na \cdot 3H_2O$ and 0.4 mass fraction of $CO(NH_2)_2$, melts congruently at 31.5 °C.

Melting-point diagrams at ambient pressure for system CH_3CO_2Na–$CO(NH_2)_2$–H_2O, in which the mass fraction of $CO(NH_2)_2$ is kept constant, are plotted in Fig. 4. In this figure, W_a shows the mass fraction of CH_3CO_2Na and W_b the mass fraction of H_2O. Therefore, the quantity on the abscissa, $100 \times W_a/(W_a+W_b)$, is the weight per cent of CH_3CO_2Na in the system with no $CO(NH_2)_2$ content. The melting-point diagram for system $CH_3CO_2Na \cdot H_2O$, which does not contain $CO(NH_2)_2$, is in good agreement with previous data.[4] It is apparent that as the mass fraction of $CO(NH_2)_2$, W_x, increases, the liquidus lines on the $CH_3CO_2Na \cdot 3H_2O$ side shift to lower temperatures and that the liquidus lines on the CH_3CO_2Na side shift to higher concentrations of CH_3CO_2Na.

A partial phase diagram of ternary system CH_3CO_2Na–$CO(NH_2)_2$–H_2O at ambient pressure is constructed by using the results of Figs. 1, 3, and 4 and shown in Fig. 5. From this figure, it is understandable that $CH_3CO_2Na \cdot 3H_2O$ comes to melt congruently when a sufficient quantity of $CO(NH_2)_2$ or H_2O is added to it. Moreover, the liquidus line on the $CH_3CO_2Na \cdot 3H_2O$ side is lowered by addition of $CO(NH_2)_2$ or H_2O. Thus, the effect of addition of

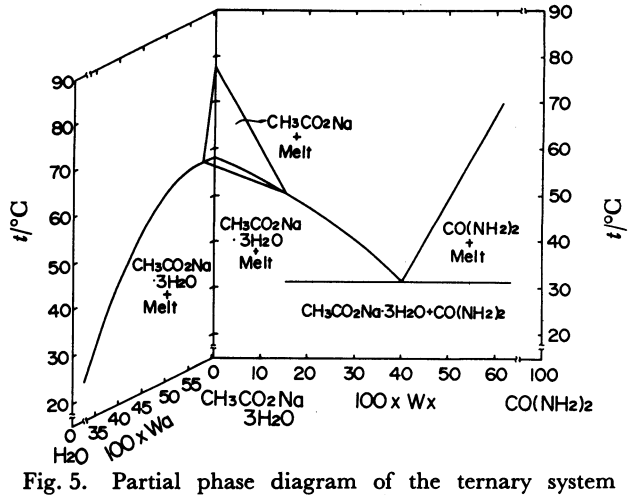

Fig. 5. Partial phase diagram of the ternary system CH_3CO_2Na–$CO(NH_2)_2$–H_2O at ambient pressure.

$CO(NH_2)_2$ to $CH_3CO_2Na \cdot 3H_2O$ is similar to that of addition of H_2O. But, the eutectic point of pseudo-binary system $CH_3CO_2Na \cdot 3H_2O$–$CO(NH_2)_2$ is 31.5 °C, which is suitable for solar energy storage, whereas the eutectic point of system $CH_3CO_2Na \cdot 3H_2O$–H_2O is −18 °C, which is too low. The reason why $CH_3CO_2Na \cdot 3H_2O$ is brought to the point of melting congruently by the addition of a sufficient quantity of $CO(NH_2)_2$ is that $CO(NH_2)_2$ acts not only as a solute in $CH_3CO_2Na \cdot 3H_2O$ melt but also as a solvent for CH_3CO_2Na like H_2O. That is to say, as an aqueous solution of $CO(NH_2)_2$ acts as a mixed solvent for CH_3CO_2Na, the solubility of CH_3CO_2Na for unit mass of H_2O is higher in the mixture of system $CH_3CO_2Na \cdot 3H_2O$–$CO(NH_2)_2$ melt than in the melt of $CH_3CO_2Na \cdot 3H_2O$ without any other substances.

The heat of fusion of the eutectic mixture of this pseudo-binary system is found to be 226 J/g by DSC. This value is larger than the heat of fusion of another latent heat storage material, $CaCl_2 \cdot 6H_2O$ (t_m: 29.5 °C), 180 J/g. The heat of fusion of a binary eutectic mixture ΔH_m^{eu} is calculated from the equation.[6]

$$\Delta H_m^{eu} = T_m^{eu}\left\{W^A\left(\frac{\Delta H_m{}^A}{T_m{}^A}\right) + W^B\left(\frac{\Delta H_m{}^B}{T_m{}^B}\right)\right\}, \quad (1)$$

where W^A and W^B are the mass fractions of components A and B, respectively, T_m^A, T_m^B, and T_m^{eu} are the melting points (in absolute temperature) of component A, component B, and eutectic mixture, respectively, and ΔH_m^A and ΔH_m^B are the heats of fusion of components A and B per unit mass, respectively. This equation is applicable to the eutectic mixture of pseudo-binary system $CH_3CO_2Na \cdot 3H_2O$–$CO(NH_2)_2$, by letting, A and B correspond to $CH_3CO_2Na \cdot 3H_2O$ and $CO(NH_2)_2$, respectively. $CH_3CO_2Na \cdot 3H_2O$ melts incongruently at 58.4 °C with a heat of fusion of 264 J/g,[7] and $CO(NH_2)_2$ melts at 133 °C with a heat of fusion of 251 J/g.[8] Accordingly we take T_m^A=332 K, T_m^B=406 K, T_m^{eu}=305 K, ΔH_m^A=264 J/g, ΔH_m^B=251 J/g, W^A=0.60, and W^B=0.40. Consequently, ΔH_m^{eu} is 221 J/g. This value is in good agreement with the experimental result, 226 J/g.

Microphotographs of mixtures of $CH_3CO_2Na \cdot 3H_2O$ and $CO(NH_2)_2$ are given in Figs. 6—8. The study with a microscope clearly proves that the solid immediately separating out from a eutectic melt is entirely different in appearance from other solids. Large prisms of $CH_3CO_2Na \cdot 3H_2O$ in the eutectic matrix are shown in Fig. 6. White needles of $CO(NH_2)_2$ in the eutectic matrix are shown in Fig. 7. An extremely regular pattern microphotographed for the solid eutectic matrix is shown in Fig. 8.

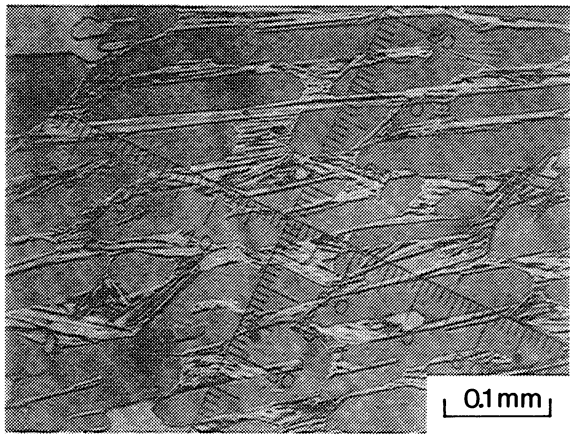

Fig. 6. Microstructure of mixture containing 0.2 mass fraction of $CO(NH_2)_2$.

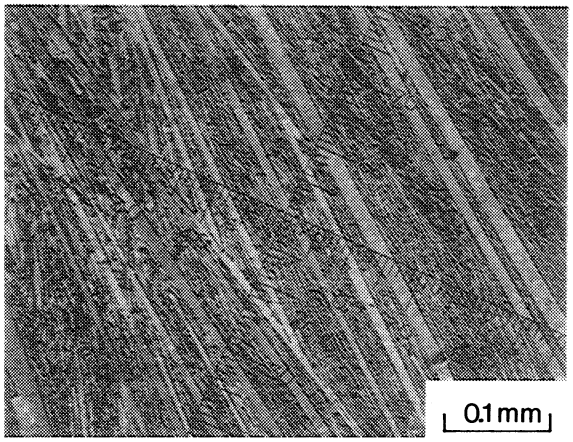

Fig. 7. Microstructure of mixture containing 0.6 mass fraction of $CO(NH_2)_2$.

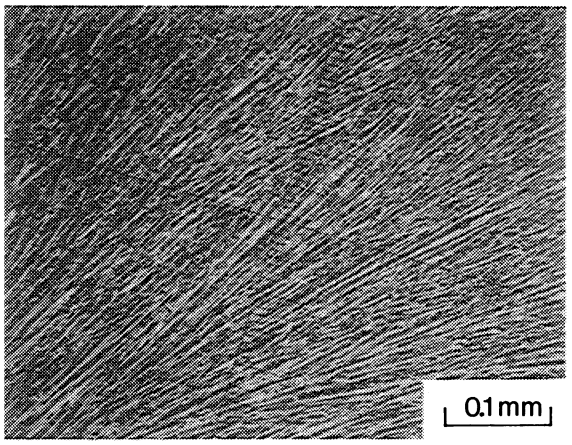

Fig. 8. Microstructure of eutectic mixture containing 0.4 mass fraction of $CO(NH_2)_2$.

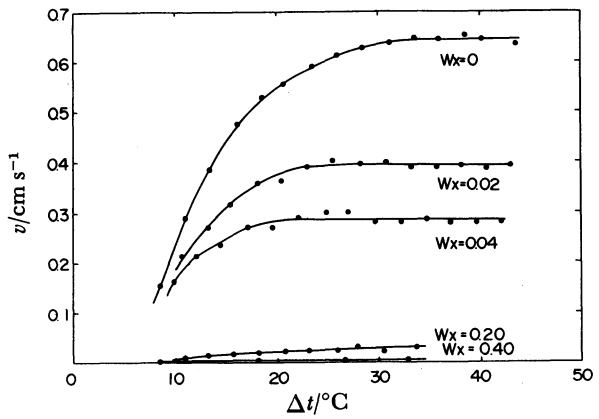

Fig. 9. Linear velocity of crystallization of various melts.

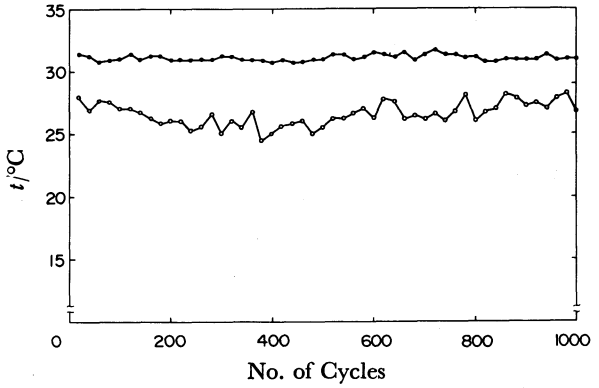

Fig. 10. Changes in melting point t_m and the temperature at which supercooling is broken t_i with cycling.
●: t_m, ○: t_i.

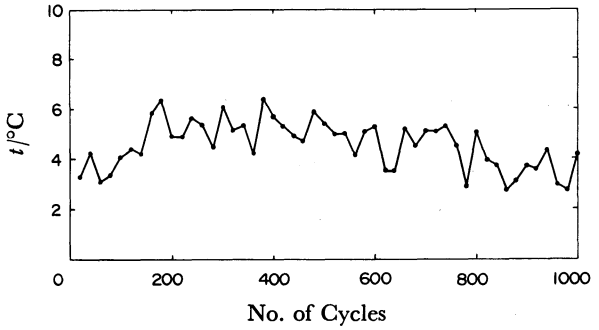

Fig. 11. Changes in supercooling Δt_i with cycling.

Linear velocities of crystallization of various melts are plotted against the supercooling Δt in Fig. 9. The linear velocity of crystallization of $CH_3CO_2Na \cdot 3H_2O$ ($W_x=0$) is in good agreement with the value determined by Dietz *et al.*[3] It is clear that the linear velocity of crystallization of the melt containing 0.04 mass fraction of $CO(NH_2)_2$ at $\Delta t=20$ °C falls to less than half the linear velocity of crystallization of $CH_3CO_2Na \cdot 3HO_2$ at $\Delta t=20$ °C. The linear velocity of crystallization of this eutectic melt at $\Delta t=20$ °C, 0.002 cm/s, is about 1/300 of the linear velocity of crystallization of $CH_3CO_2Na \cdot 3H_2O$ melt at $\Delta t=20$ °C.

To make sure that the mixture of system $CH_3CO_2Na \cdot 3H_2O$–$CO(NH_2)_2$ continuously repeats stable freezing, 30 g of the eutectic mixture of pseudo-binary system $CH_3CO_2Na \cdot 3H_2O$–$CO(NH_2)_2$, in the presence of 0.3 g of $Na_4P_2O_7 \cdot 10H_2O$ as the nucleation catalyst for $CH_3CO_2Na \cdot 3H_2O$, was subjected to cycles of linearly programmed consequtive heating and coolings between 5 and 45 °C in a manner similar to the one adopted previously.[9] Melting points t_m's and temperatures at which the supercooling is broken, t_i's as determined by 1000 continuous heating and cooling cycles, are shown in Fig. 10. The supercooling $\Delta t_i(=t_m-t_i)$ is calculated by using the results in Fig. 10 and plotted in Fig. 11. From these figures, it is apparent that the supercooling of this eutectic mixture Δt_i is almost 6 °C for all the cycles.

$CH_3CO_2Na \cdot 3H_2O$ starts to crystallize from the eutectic melt with the aid of $Na_4P_2O_7 \cdot 10H_2O$ crystals and soon $CO(NH_2)_2$ starts to crystallize. This eutectic mixture was observed not to separate into the components $CH_3CO_2Na \cdot 3H_2O$ and $CO(NH_2)_2$. After 1000 continuous heating and cooling cycles, the heat of fusion of this sample was measured by DSC. The value obtained is 222 J/g, which is in good agreement with the initial heat of fusion of this eutectic mixture, 226 J/g. Consequently, the mixtures of system $CH_3CO_2Na \cdot 3H_2O$–$CO(NH_2)_2$ are promising for solar energy storage.

The authors wish to express their thanks to Dr. Ryoichi Kiriyama for his helpful discussions and to Drs. Eiichi Hirota and Masanari Mikoda for their continuous encouragement. They are also grateful to Dr. Yoshihiro Matsuo for his discussions throughout this work.

References

1) K. W. Böer, J. H. Higgins, and J. K. O'Connor, IECEC '75 Record, 7 (1975).
2) N. Yoneda and S. Takanashi, *Solar Energy*, **21**, 61 (1978).
3) P. L. Dietz, Jr., J. S. Brukner, and C. A. Hollingsworth, *J. Phys. Chem.*, **61**, 944 (1957).
4) W. F. Green, *J. Phys. Chem.*, **12**, 655 (1908).
5) B. Carlsson, H. Stymne, and G. Wettermark, *Solar Energy*, **23**, 343 (1979).
6) M. Kaminoto, T. Tanaka, T. Tani, and T. Horigome, *Solar Energy*, **24**, 581 (1980).
7) M. Telkes, "Solar Materials Science," ed by L. E. Murr, Academic Press, New York (1980), Chap. 11.
8) T. Ozawa, M. Kamimoto, R. Sakamoto, Y. Takahashi, and K. Kanari, *Bull. Electrotech. Lab.* **43**, 19 (1979).
9) T. Wada and R. Yamamoto, *Bull. Chem. Soc. Jpn.*, **55**, 3603 (1982).